

NORDITA - 96/49 N,P  
hep-ph/9607460

# Neural Network analysis for $\gamma\gamma \rightarrow \pi^+\pi^-\pi^0$ at Daphne<sup>1</sup>

Ll. Ametller<sup>a</sup>, Ll. Garrido<sup>b,c</sup> and P. Talavera<sup>d</sup><sup>2</sup>

<sup>a</sup>Departament de Física i Enginyeria Nuclear  
Universitat Politècnica de Catalunya, E-08034 Barcelona, Spain

<sup>b</sup>Departament Estructura i Constituents Matèria  
Universitat de Barcelona, E-08028 Barcelona, Spain

<sup>c</sup>Institut de Física d'Altes Energies  
Universitat Autònoma de Barcelona, E-08193 Bellaterra (Barcelona), Spain

<sup>d</sup> NORDITA, Blegdamsvej 17, DK-2100, Copenhagen Ø, Denmark

## Abstract

We consider the possibility of using neural networks in experimental data analysis in Daphne. We analyze the process  $\gamma\gamma \rightarrow \pi^+\pi^-\pi^0$  and its backgrounds using neural networks and we compare their performances with traditional methods of applying cuts on several kinematical variables. We find that the neural networks are more efficient and can be of great help for processes with small number of produced events.

---

<sup>1</sup>This research is partly supported by EU under contract number CHRX-CT92-0004 and by the Comissionat per Universitats i Recerca de la Generalitat de Catalunya.

<sup>2</sup>Supported by EU under contract number ERB 4001GT952585.

# 1 Introduction

The Daphne  $\Phi$ -factory should start to operate very soon in Frascati. Its main goals are the study of  $\Phi$  decays and related processes, mainly studies of CP violation in kaon decays,  $\pi-\pi$  phase shifts,  $\eta$  decays, etc. [1] Being an  $e^+ e^-$  collider, the machine is also suited to study  $\gamma\gamma$  physics. In this context, the golden plate process at Daphne is  $\gamma\gamma \rightarrow \pi^0\pi^0$ . The main reason is that the present experimental situation is not well established, at least at the region near threshold, where good theoretical predictions exist in the context of Chiral Perturbation Theory (ChPT). Moreover, this theoretical predictions start at the one-loop level, and thus this process is a clear test of the effective quantum field theory character of ChPT. In a similar way, other interesting processes have been proposed recently. In particular, the processes  $\gamma\gamma \rightarrow 3\pi$  are also interesting because one-loop predictions dominate over tree-level ones [2]. They differ however from  $\gamma\gamma \rightarrow \pi^0\pi^0$  in several aspects: i) They are anomalous processes, ii) they are not exclusive test of chiral loops since they get contributions from counterterms and iii) their cross sections are much smaller, thus more difficult to measure experimentally. The best way consists in tagging the electron and positron, but at expenses of reducing significantly the number of events due to small tagging efficiencies [3]. It is therefore convenient to dispose of alternative methods with large efficiency and without lepton tagging whenever possible. We suggest that neural networks (NN's) could be used in experimental analysis for such a purpose. We have trained a NN with  $\gamma\gamma \rightarrow \pi^+\pi^-\pi^0$  (signal) and have considered the three main sources of background. Our analysis avoids tagging (thus we are not penalized by small tagging efficiencies) and obtains results which are better than traditional methods based in applying cuts over a set of kinematical variables.

This work is organized as follows. In section 2 we describe briefly ChPT and its predictions for  $\gamma\gamma \rightarrow 3\pi$  at Daphne. Section 3 gives a short description of NN's. In Section 4 we describe the generation of data for the signal and the analyzed backgrounds and introduce the set of kinematical variables which are used as the NN inputs. The performance of the NN is compared with the usual methods of analysis in Section 5. Section 6 is devoted to the conclusions.

## 2 Chiral Perturbation Theory for $\gamma\gamma \rightarrow 3\pi$

ChPT is an effective formulation of QCD at low energy in terms of pseudoscalar mesons as fundamental fields[4]. It is inspired from QCD enforcing its symmetry properties. Indeed, the QCD Lagrangian –in terms of quarks and gluons– possesses a Chiral  $SU(3)_L \times SU(3)_R$  symmetry, for massless quarks. However, when considering the quark mass terms, these break the chiral symmetry. In the effective low energy version of QCD, one replaces the fundamental quark and gluon fields by the pseudoscalar mesons, imposing  $SU(3)_L \times SU(3)_R$  symmetry, only broken by terms proportional to the quark masses, which can be related to the pseudoscalar meson masses. The ChPT Lagrangian can be written as an expansion in momenta and masses and treated perturbatively. The first order ChPT predictions

are essentially equivalent to Current Algebra. However, they get corrections from higher order terms, playing loops a particular role. They are essential in order to incorporate the correct analyticity, unitarity and crossing symmetry properties of the physical amplitudes. Moreover, loops give –in general– divergences which can only be absorbed by tree-level counterterms present in the higher order Lagrangian. The number of needed counterterms depends on the order of the momentum expansion. This is a consequence of the non renormalizability of the theory (in the classical sense that all divergences can be absorbed in a fixed, finite, number of terms). In spite of that, the theory can still give predictions provided one can fix the values of the counterterms through related processes. When this is not possible, one has to rely on some phenomenological models to estimate those counterterms, but at expenses of introducing model dependence in the game. Electroweak interactions can be introduced in a systematic and selfconsistent way.

One distinguishes two sectors in ChPT. The normal, even intrinsic parity sector, treats processes as, for instance,  $\pi\pi \rightarrow \pi\pi$ ,  $\eta \rightarrow 3\pi$ , or  $\gamma\gamma \rightarrow \pi\pi$ . The anomalous, odd intrinsic parity sector, accounts for processes as  $\pi^0 \rightarrow \gamma\gamma$ ,  $\eta \rightarrow \pi\pi\gamma$ , and  $\gamma\gamma \rightarrow 3\pi$ . From the former sector, the  $\gamma\gamma \rightarrow \pi^0\pi^0$  process plays an important role. This is because there is no tree level contribution [5]. The first non vanishing contribution starts at  $O(p^4)$  –in the momentum expansion– and is entirely given by one loop diagrams, with no contribution from the  $O(p^4)$  tree level Lagrangian. This makes the process very interesting, since it tests the loop predictions of the theory. In a similar way, the anomalous processes  $\gamma\gamma \rightarrow 3\pi$  receive contributions from  $O(p^6)$  which dominate over the non vanishing tree level ones and test the loop predictions in the anomalous sector, although in a less severe way, since there are two types of  $O(p^6)$  contributions, loops and counterterms.

In Refs.[2, 6] the amplitudes for  $\gamma\gamma \rightarrow \pi^+\pi^-\pi^0$  and  $\gamma\gamma \rightarrow 3\pi^0$  have been obtained with the corresponding predictions for the expected number of events at Daphne. One expects around 180 (23) events per year for the first (second) process. These are quite moderate number of events, and require good strategies for its eventual experimental detection. We suggest that using NN's can be a good possibility to perform an efficient analysis. We restrict our analysis to the first, charged channel, which looks a priori more promising than the neutral one.

### 3 Neural Networks

Neural Networks (NN's) are useful tools for pattern recognition. In high energy physics, they have been used or proposed as good candidates for tasks of signal versus background classification. Some examples are the Higgs searches [7], b and  $\tau$  analysis [8], quark and gluon jets analysis [9], determination of Z to heavy quarks branching ratios [10], bottom-jet recognition [11] and top-quark search in  $p\bar{p}$  colliders [12, 13]. Recently, NN's have been used for experimental top quark searches at the Tevatron[14].

We have considered layered feed-forward NN's with topologies  $N_i \times N_{h_1} \times N_{h_2} \times N_o$ , where  $N_i$  ( $N_o$ ) are the number of input (output) neurons and  $N_{h_1}, N_{h_2}$  are the neurons in two hidden layers.

The input of neuron  $i$  in layer  $l$  is given by,

$$I_i^l = in_i^{(e)}, \quad l = 1 ; \quad I_i^l = \sum_j w_{ij}^l S_j^{l-1} + B_i^l, \quad l = 2, 4 , \quad (1)$$

where  $in_i^{(e)}$  is the set of kinematical variables describing a physical event  $e$ , the sum is extended over the neurons of the preceding layer ( $l - 1$ ),  $S_j^{l-1}$  is the state of the neuron  $j$ ,  $w_{ij}^l$  is the connection weight between the neuron  $j$  and the neuron  $i$ , and  $B_i^l$  is a bias input to neuron  $i$ . The state of a neuron is a function of its input  $S_j^l = F(I_j^l)$ , where  $F$  is the neuron response function. In this study the “sigmoid function”,  $F(I_j^l) = 1/(1 + \exp(-I_j^l))$ , has been chosen. This function offers a more sensitive modeling of real data than a linear one.

Back-propagation was used as the learning algorithm. Its main objective is to minimize the quadratic output-error  $E$ ,

$$E = E(in_i^{(e)}, out^{(e)}, w_{kl}, B_k) = \frac{1}{2} \sum_e (o^{(e)} - out^{(e)})^2 . \quad (2)$$

This minimization is obtained by adjusting the  $w_{kl}$  and  $B_n$  parameters, where  $o^{(e)}$  is the state of the output neuron for event  $e$ ,  $out^{(e)}$  is its desired state, and  $e$  runs over the learning sample. Taking the desired output as 1 for signal events and 0 for background events, the network output gives, after training, the conditional probability that new test events presented to the network are of signal- or background-type [15], provided that the signal/background ratio used in the learning phase corresponds to the real one.

Weights are updated for each event presented to the NN during the learning phase. Once the quadratic error  $E$  reaches its minimum value, they are kept fixed and used in the testing phase where the NN is used as a signal–background classifier. A frequent problem encountered in NN training is over-learning. It takes place when the NN interprets statistical fluctuations as real differences. In this study over-learning is avoided by checking the evolution of the error on a test sample,  $E_t$ , and stop learning when  $E_t$  starts to increase, even if the learning error function  $E$  still continues to decrease.

## 4 Data generation for signal and backgrounds

We take as signal in our analysis the process  $\gamma\gamma \rightarrow \pi^+\pi^-\pi^0$  as predicted by ChPT at  $O(p^6)$  [6] in Daphne, running at  $e^+e^-$  center of mass energies  $\sqrt{s} = M_\Phi$ . We avoid tagging of the leptons for its analysis, in order to keep all produced events. In so doing, we had to consider several types of backgrounds. We analyzed the following ones:

- B1)  $\gamma\gamma \rightarrow \eta \rightarrow \pi^+\pi^-\pi^0$
- B2)  $e^+e^- \rightarrow \omega, \Phi \rightarrow \pi^+\pi^-\pi^0\gamma$
- B3)  $e^+e^- \rightarrow (\omega, \Phi)\gamma \rightarrow \pi^+\pi^-\pi^0\gamma$

The first background B1 is eta photoproduction. It has the same origin as the signal and differs from it because the invariant mass of the three pion system is strongly peaked around the eta mass. The background B2 consists in the decay of a real (virtual)  $\Phi$  ( $\omega$ ) vector meson which decays into  $\pi^+\pi^-\pi^0\gamma$ . The background B3 accounts for virtual production of  $\Phi$  or  $\omega$  vector mesons and one initial state bremsstrahlung photon. In the last two processes, we demand the presence of one undetected photon. This photon decreases the available energy of the three-pion system and eliminates the production and decay of a virtual  $\omega$  into  $3\pi$  as potential background. The photon escapes detection mainly going through the beam pipe.

As it has been previously mentioned, the signal has been predicted in the context of ChPT. The first background has been estimated in the same context, but using a constant matrix element evaluated at the center of the Dalitz plot. This is a good approximation for our purpose of estimating the range of energies where this background is important. The backgrounds B2 and B3 have been computed using vector meson dominance.

We have generated Monte Carlo events for the signal and the backgrounds, satisfying the following generation cuts:

- 1) All pions are in the detector, which has almost full  $4\pi$  acceptance except for the beam pipe, which corresponds to a fraction of 2% of the total solid angle.
- 2) The invariant mass of the three pion state is restricted to be in the range  $3m_\pi \leq m_{3\pi} \leq 0.7$  GeV. The upper limit is conservatively taken in such a way that the ChPT matrix elements used for the signal and the background B1, computed at  $O(p^6)$ , can be trusted. For larger invariant masses, one expects that higher order corrections could be important and modify significantly the estimation of the signal.
- 3) The photons produced in backgrounds B2 and B3, escape detection through the beam pipe. On the contrary, they should be easily detected since their energy is forced to be in the range  $255 \text{ MeV} \leq E_\gamma \leq 341 \text{ MeV}$  due to the above constraint imposed on  $m_{3\pi}$ .
- 4) As we are interested in a final  $3\pi$  state not coming from  $\eta$  production, we make an additional cut on  $m_{3\pi}$ . We demand  $m_\eta + \Delta \leq m_{3\pi} \leq m_\eta - \Delta$ . Taking  $\Delta = 20$  MeV, the first background is practically eliminated [6], since it is only important around the  $\eta$  mass region.

The number of expected events per year passing the generation cuts for the Daphne integrated luminosity of  $\int L dt = 5 \times 10^6 \text{ nb}^{-1}$  are: 71, 0.07, 1714, 776 for the signal and each of the backgrounds, respectively. The background B1 can be safely discarded.

For the analysis and as inputs to the NN, we chose the following kinematical variables

- 1) The  $\pi^+$  transverse momentum,
- 2) the  $\pi^-$  transverse momentum,
- 3) the  $\pi^0$  transverse momentum,
- 4) the three pion system transverse energy,
- 5) the  $\pi^+$  pseudorapidity,

- 6) the  $\pi^-$  pseudorapidity,
- 7) the  $\pi^0$  pseudorapidity,
- 8) the three pion system sphericity in the three pion center of mass,
- 9) the difference between  $m_\rho$  and its best approximation by the invariant masses of all possible pairs of pions.

All the above variables are self explained, except the last one which was chosen because background B3 is mediated by a  $\rho$  exchange with its subsequent decay into a pion pair. There is no need to say that one could have considered other variables, as angular correlations among the final pions, for example, which bring additional information on the physics of the process and could help in the task of signal versus background separation.

## 5 Results

Rather than using the expected number of events produced at Daphne, we generated bigger samples of 10000 signal, B2 and B3 background events, passing the generation cuts. From each of those, 8000 events were used to train a  $(N_1 = 9) \times (N_{h_1} = 11) \times (N_{h_2} = 5) \times (N_o = 1)$  NN –denoted by NN9 from now on– to give output 1 for the signal and 0 for the backgrounds. The rest of events were reserved for doing the NN test and the analysis in a classical way. (The B1 background is eliminated by the generation cut 4.) The obtained results were rescaled to the expected number of events produced at Daphne per year. In Fig. 1 we show the distribution of the test events that survive as a function of the NN9 output cut. (An event survives if its corresponding output is larger than the chosen output cut.) The dot-dashed (solid) line corresponds to the signal (total background) events. One can deduce that the signal events are very peaked to output values very close to one, while the background events tend to concentrate at values close to zero. It is clear that one can select subsamples richer on signal or background with suitable choices of NN output cuts. In our case, we are interested in improving the signal to background ratio, thus we will accept events with outputs larger than a given output cut. A good variable to parametrize the efficiency of the analysis is the statistical significance, defined as  $S_s = N_s / \sqrt{N_b}$ , being  $N_s$  ( $N_b$ ) the number of signal (background) accepted events. The solid line in Fig. 2 shows the statistical significance  $S_s$  as a function of the NN9 output cut. The curve has been plotted for output cut values up to 0.95, to avoid strong fluctuations on its estimation due to lack of statistics. For output cuts around 0.9, the achievable  $S_s$  is around 60, thus indicating that the NN performs a very good job in the signal recognition against the considered backgrounds.

At this point, we would like to stress the benefits of using the NN over more traditional methods of doing the experimental analysis. Indeed, usually experimentalists perform several cuts on some kinematical variables to isolate the regions where the signal differs most from the backgrounds. This procedure, when one considers a large number of variables, is

usually done by means of linear cuts, isolating hypercubical regions in favor of the signal. Its efficiency is known to be lower than the achievable by NN techniques [12]. One can wonder, however, how the NN results compare with smarter ways of applying cuts. In particular, it is clear that one has to isolate regions of the parameter space with complicated geometry, so linear cuts will have limited success in general. One has to consider non linear cuts specially designed by previous inspection of the signal and background. This is only feasible, in practice, for small number of variables in the analysis. We performed an analysis in these terms using the three most significant variables. These were obtained from the nine original variables using the methods discussed in Ref. [13], involving the weights connecting the inputs with the first hidden layer. They turned to be the pseudorapidities of the pions. The topology of the signal and background events in the three pseudorapidities space look qualitatively different. The signal tends to lie inside an ellipsoidal surface centered at the origin, while the background events are preferably distributed into two separated regions, symmetrically located respect to the origin.

We could isolate non linear regions with statistical significances up to 10. Notice that this result must not be compared with the results of the NN9, which were obtained using the full set of the original 9 variables. In order to do a fair comparison, we trained a smaller NN using the same three input variables, which we denote by NN3, with topology  $(N_1 = 3) \times (N_{h_1} = 5) \times (N_{h_2} = 5) \times (N_o = 1)$ . The results of this NN3 net are also shown in the figures. The dotted (dashed) line in Fig. 1 shows the accumulated number of signal (background) events as a function of the NN3 output cut. The reconstruction of the signal is fairly good, but the background is much worse respect to the NN9. This translates into much smaller statistical significances, typically by a factor of 6, as it is shown by the dashed line of Fig. 2, where  $S_s$  is plotted as a function of the NN3 output cut.

Two comments are in order. First, notice that we were interested in reducing the variables to three, to be able to design good sets of non linear cuts with the help of three dimensional distributions of events. In case of keeping more variables, the statistical significances would not be so drastically reduced. Second, the reduced NN3, for output cuts larger than 0.85, is at least as efficient as the best optimized non linear classical cuts we could find. Moreover, there is a great advantage of the NN3 in front of the non linear cuts: Whereas the latter have to be designed by visual inspection and require dedicated work, the NN operates in a completely automatic way, with comparable efficiency. This is not surprising. It is due, in fact, to the highly non linear behaviour of the NN's, which allows them to select complicated regions of the parameter space in an automatic and painless way.

Finally, NN's can be easily trained for any number of input variables. On the contrary, non-linear classical analyses are strongly limited to small number of variables. This makes NN's very useful tools for processes where high efficiencies are needed.

## 6 Conclusions

We have considered the ability of NN's to perform experimental analysis for the process  $\gamma\gamma \rightarrow \pi^+\pi^-\pi^0$  at Daphne. The ChPT prediction for the number of events produced is relatively small, thus indicating that efficient methods for its detection and analysis can be of great help. We have considered three types of backgrounds which mimic the signal and we have avoided tagging of the initial leptons which would imply a sensible reduction of event statistics. Using a set of nine kinematical variables as inputs of a NN9, we have obtained large statistical significances for a wide interval of output cuts.

We have also studied the expected efficiencies for a smaller NN3, using the three pion pseudorapidities as inputs, and compared them with the efficiencies found by using classical analyses in terms of non linear cuts for the same variables. We have found that the NN3 statistical significances, obtained in an automatic and painless way, are at least as good as the best result we could find using non linear cuts chosen through accurate inspection on the distribution of the signal and background events in the three variable space. This is due to the highly non linear behaviour of the NN, which isolates the phase space regions where the signal differs significantly from the background. However, the NN3 efficiency is much smaller than the one obtained by NN9. It is therefore highly recommended to use large sets of kinematical variables for ensuring large efficiencies. This represents no extra effort for the NN's and can be a great challenge for classical methods. We finally stress that the usefulness of NN's is not restricted to the signal analysed, but it can be shown to work similarly for any other process of interest.

### Acknowledgements

We thank A. Bramon and J. Bijnens for useful discussions.

## References

- [1] “The second Daphne physics handbook” edited by L. Maiani, G. Pancheri and N. Paver, publication INFN-LNF (1995).
- [2] P. Talavera et al., Phys. Lett. B 376 (1996) 186.
- [3] G. Alexander et al., Nuovo Cimento **107** A (1994) 837.
- [4] See for example J. Bijnens, G. Ecker and J. Gasser in [1], page 125 and references there in.
- [5] J. Bijnens and F. Cornet, Nucl. Phys. B **296** (1988) 557.
- [6] Ll. Ametller et al, in preparation.

- [7] P. Chiapetta, P. Colangelo, P. de Felice, G. Nardulli and G. Pasquariello, Phys. Lett. B **322**, 219 (1994); G. Stimpfl-Abele and P. Yepes, Comput. Phys. Commun. **78**, 1 (1993).
- [8] V. Innocente, Y. F. Wang and Z. P. Zhang, Nucl. Instr. Meth. A **323**, 647 (1992).
- [9] M. A. Graham, L. M. Jones and S. Herbin, Phys. Rev. D **51**, 4789 (1995).
- [10] N. de Groot, Amsterdam Univ., Ph. D. Thesis 1993.
- [11] P. Mazzanti and R. Odorico, Z. Phys. C **59**, 273 (1993); K. H. Becks, F. Block, J. Drees, P. Langefeld and F. Seidel, Nucl. Instrum. Meth. A **329**, 501 (1993).
- [12] H. Baer, D. Dzialo Karatas and G. F. Giudice, Phys. Rev. D **46**, 4901 (1992); Ll. Ametller, Ll. Garrido and P. Talavera, Phys. Rev. D **50**, R5473 (1994).
- [13] Ll. Ametller et al., Phys. Rev. D **54** (1996) 1233.
- [14] P. C. Bhat, in the Albuquerque meeting, Proceedings of the Meeting of the Division of Particles and Fields of the APS, Albuquerque, New Mexico, 1994, edited by S. Seidel (World Scientific, Singapore, 1995); Fermilab-Conf-95/211-E (unpublished).
- [15] Ll. Garrido and V. Gaitan, Int. J. Neural Sys. **2**, 221 (1991); V. Gaitan Alcalde, Universitat Autònoma de Barcelona, Ph. D. Thesis, 1993; S. Gómez and Ll. Garrido, Int. J. Neural Sys. **7** (1996) N.1; D.W. Ruck et al., IEEE Transactions on Neural Networks, **1**, 296 (1990); E.A. Wan, IEEE Transactions on Neural Networks, **1**, 303 (1990).

## List of Figures

1	Accumulated number of events with output larger than a given output cut.	10
2	Statistical significance as a function of the NN output cut. . . . .	11

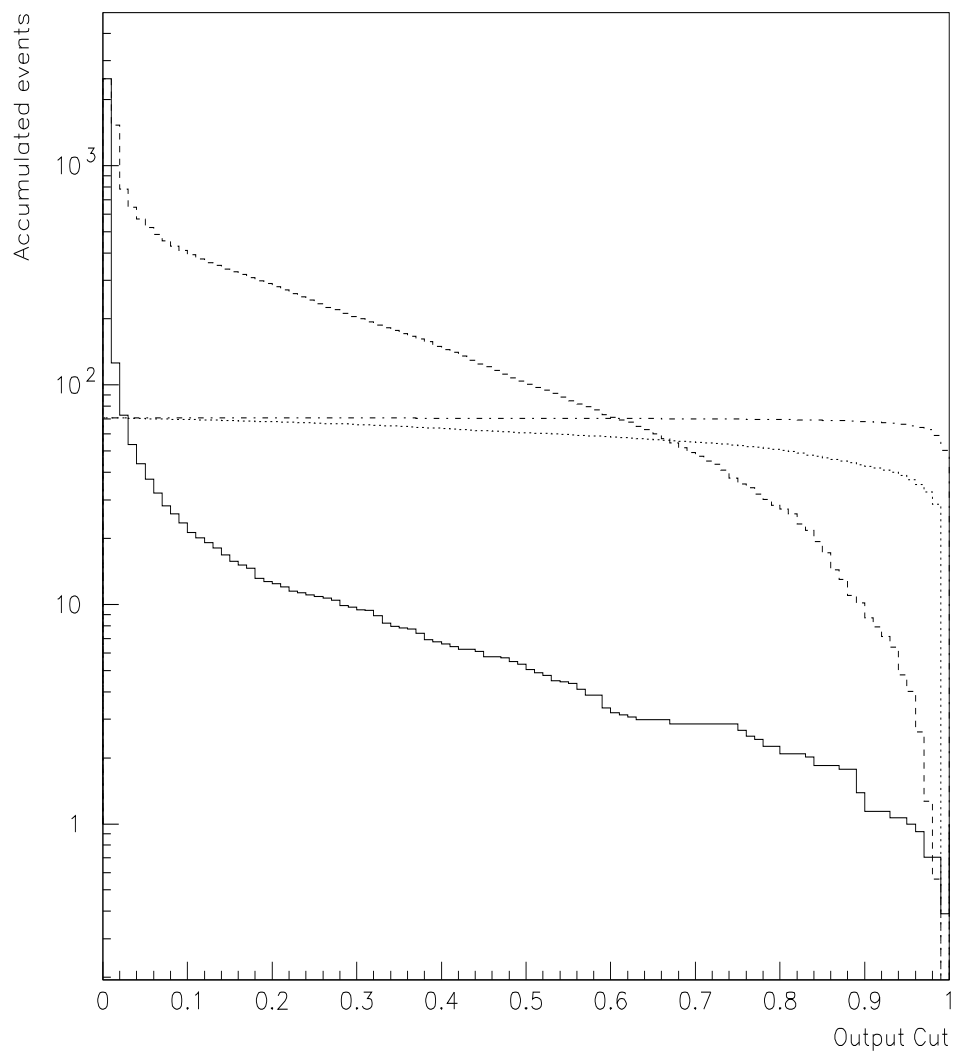


Figure 1: Accumulated number of events with output larger than a given output cut. Solid (dashed) and dot-dashed (dotted) lines correspond to the background and signal results, respectively, for NN9 (NN3).

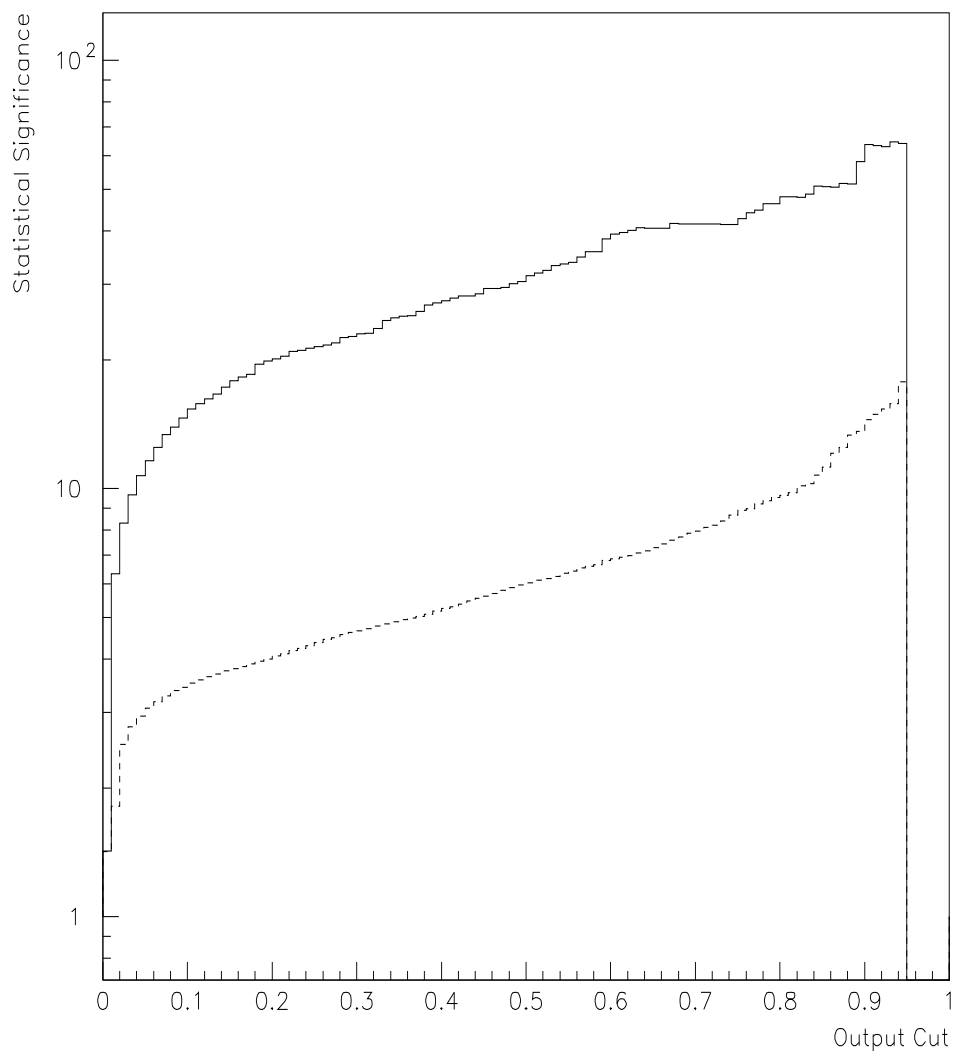


Figure 2: Statistical significance as a function of the NN output cut. Solid (dashed) line corresponds to the NN9 (NN3) net.